HST multi-epoch imaging of the PSR B0540-69 system unveils a highly dynamic synchrotron nebula.[1]

A. De Luca

INAF - Istituto di Astrofisica Spaziale e Fisica Cosmica, Via Bassini 15, I-20133 Milano, Italy

deluca@iasf-milano.inaf.it

and

R.P. Mignani

University College London, Mullard Space Science Laboratory, Holmbury St. Mary, Dorking, Surrey, RH5 6NT United Kingdom

and

P.A. Caraveo

INAF - Istituto di Astrofisica Spaziale e Fisica Cosmica, Via Bassini 15, I-20133 Milano, Italy

and

G.F. Bignami[1]

Agenzia Spaziale Italiana, Via Liegi 26, I-00198 Roma, Italy

ABSTRACT

PSR B0540-69 is the Crab twin in the Large Magellanic Cloud. Age, energetic and overall behaviour of the two pulsars are very similar. The same is true for the general appearance of their pulsar wind nebulae (PWNe). Analysis of Hubble Space Telescope images spanning 10 years unveiled significant variability in the PWN surrounding PSR B0540-69, with a hot spot moving at $\sim$ 0.04c. Such behaviour, reminiscent of the variability observed in the Crab nebula along the counter-jet direction, may suggest an alternative scenario for the geometry of the system. The same data were used to assess the pulsar proper motion. The null displacement recorded over 10 y allowed us to set a 3σ upper limit of 290 km s^{-1} to the pulsar velocity.

[1]Istituto Universitario di Studi Superiori di Pavia, Via Luino 4, 27100 Pavia, Italy

Subject headings: stars: neutron — pulsars: individual (PSR B0540-69)

1. Introduction

PSR B0540-69 in the Large Magellanic Cloud (LMC) is one of the youngest pulsars known to date[2] (characteristic age $\tau \sim 1600$ years) and one of the very few first observed at wavelengths other than radio. It was discovered in X-rays by the *Einstein Observatory* (Seward et al. 1984), soon detected to pulsate in the optical (Middleditch & Pennypacker 1985), but detected in radio only 10 years later (Manchester et al. 1993). PSR B0540-69 is a fast ($\sim$ 50 ms), classical pulsar with a rotational energy loss very similar to that of the Crab ($\sim 1.5 \times 10^{38}$ erg s^{-1}). Thus, the detection of a polarized plerion-like structure (Chanan & Helfand 1990) came as no surprise, making it the most Crab-like of the Crab-like remnants.

With the first high resolution optical images of the field (Caraveo et al. 1992) it was possible to identify the pulsar optical counterpart (V $\sim$ 22.6), disentangling it from the surrounding structured plerion. This picture was confirmed by a snapshot Hubble Space Telescope (HST) observation (Caraveo et al. 1998) which clearly resolved, within $\sim 4''$ from the pulsar, the plerion, elongated in the northeast-southwest direction.

Using early Chandra data, Gotthelf & Wang (2000) and Kaaret et al. (2001) performed a morphological study of the plerion in the X-ray band and found a noticeable similarity (accounting for different distance) with the Crab pulsar-wind nebula (PWN). Furthermore, Gotthelf & Wang (2000) unveiled the presence of a brighter PWN region south-west of the pulsar. Somehow in analogy with the Crab case, they suggested such region to belong to a torus around the source, since it appears perpendicular to a much fainter structure protruding from the pulsar and tentatively identified as a jet.

Caraveo et al. (2000) performed a multiwavelength analysis of the PSR B0540-69 PWN morphology by superimposing Chandra and HST images, finding a good correlation between the optical and X-ray structures with the PWN emission enhanced in both cases SW of the pulsar, i.e. along the putative torus proposed by Gotthelf & Wang (2000).

More recently, detailed studies of the system, based on both narrow and wide-band HST

---

[1]Based on observations with the NASA/ESA Hubble Space Telescope, obtained at the Space Telescope Science Institute, which is operated by AURA, Inc. under contract No. NAS 5-26555.

[2]see http://www.atnf.csiro.au/research/pulsar/psrcat/

observations (Serafimovich et al. 2004; Morse et al. 2006), further strenghtened the similarity with the Crab owing to the presence of a cage of filamentary ejecta possibly originating, at least in part, in a pre-supernova mass ejection phase (Caraveo et al. 1998). The complex interaction between the PWN and such envelope is dominating the plerion multiwavelength morphology, as confirmed by Petre et al. (2007), based on the analysis of a deep Chandra observations.

Interestingly, Serafimovich et al. (2004), using two HST images taken ~ 4 years apart, reported a tentative pulsar proper motion measurement of 4.9 ± 2.3 mas y^{-1} (for a pulsar projected velocity of 1190 ± 560 km s^{-1}), aligned with the putative southern jet of the PWN. This would make PSR B0540-69 the third pulsar, after the Crab (Caraveo & Mignani 1999; Ng & Romani 2006) and Vela (Caraveo et al. 2001; Dodson et al. 2003) pulsars, with a proper motion aligned with its PWN jet and, possibly, with the spin axis, which would have important consequences for pulsar kick models as well for the studies of the pulsar/PWN interactions.

In this Letter, we report the results of our analysis of the extended PSR B0540-69 HST archived dataset which allowed us to study possible morphological changes in the PSR B0540-69 PWN and to assess the pulsar proper motion over a longer time baseline.

2. HST data analysis and results

Recent HST observations of PSR B0540-69 were performed on 2005, November 15^{th} with the Wide Field and Planetary Camera 2 (WFPC2), using the wide band F555W (480 s) and the medium band F547M (1040 s) filters. Such data add up to WFPC2 observations collected in 1995 and in 1999 with several different filters (see Morse et al. 2006, for a log of the observations). In order to study the PWN variability as well as the pulsar proper motion an accurate superposition of multi-epoch data is required. We decided as a first step to use only the observations performed using the F555W filter, having a better signal to noise. Moreover, the significant WFPC2 geometric distortion, crucial for a correct proper motion measurement, has been accurately mapped for the F555W filter (Anderson & King 2003). The selected dataset, which also provides a time baseline of $\gtrsim 10$ years, includes the recent 2005 observation, as well as the original 1995, October 19^{th} (600 s) one (Caraveo et al. 1998).

The data were retrieved from the ST-ECF archive and reprocessed on-the-fly using the most appropriate reference files. Data reduction and analysis was performed using the IRAF/STSDAS, Midas and FTOOLS packages. Individual frames collected during each visit

were combined to remove cosmic rays hits, and averaged. Residual cosmic ray traces were removed using specific algorithms within Midas.

In order to register the frames, we followed the procedure we already applied in several previous astrometric works with HST (see e.g. Caraveo et al. 1996; De Luca et al. 2000; Mignani et al. 2000; Caraveo et al. 2001). A relative reference frame was defined for each image, selecting a sample of good (well resolved, not saturated, not extended, not too close to the CCD border) reference sources. In the crowded field of PSR B0540-69, 85 good sources were identified. Their position was evaluated fitting a 2-D gaussian function to their intensity profile, with a resulting uncertainty of 0.02-0.06 pixel per coordinate. The position of the pulsar optical counterpart was evaluated in the same way, with an uncertainty of order 0.03-0.04 pixel per coordinate. The coordinates of the reference stars and of the pulsar were then corrected for the WFPC2 geometric distortion using the mapping of Anderson & King (2003), as well as for the "34^{th} row" defect (Anderson & King 1999).

Next, the 1995 reference grid was assumed as a reference and was aligned along Right Ascension and Declination according to the telescope roll angle. Then, we computed the best plate transformation (accounting for independent shift and scale factor for each axis, as well as for a rotation angle) between the two grids of reference stars. We applied an iterative clipping routine, to discard reference stars yielding larger residuals. After rejecting 15 stars, we obtained a very good frame superposition, with rms uncertainties of 0.06 pixel per coordinate.

2.1. Proper motion of the pulsar

The 2005 pulsar position was translated to the 1995 reference frame, to compute the pulsar displacement over the 10.1 year time span. Such a displacement turned out to be of 0.01±0.09 pixel in R.A. and of 0.02±0.08 pixel in Dec, i.e. statistically null. Using the well calibrated WFPC2 plate scale, we set a 3σ upper limit to the source proper motion of ~ 1.7 mas yr^{-1}. At the known pulsar distance (51 kpc), such a limit corresponds to an upper limit to the total pulsar velocity (projected on the plane of the sky) of ~ 410 km s^{-1}.

As a further check, we included in our astrometric analysis the WFPC2 observations performed through the F547M filter on 2005, November 15^{th} and on 1999, October 17^{th} (800 s). Indeed, the F547M filter (pivot wavelength 5483Å, $\Delta\lambda = 483$Å FWHM) has a narrower bandpass than the F555W one (pivot wavelength 5439Å, $\Delta\lambda = 1228$Å FWHM), but the pivot wavelength is essentialy the same. Thus, the wavelength dependence of the geometric distortion should not induce any bias when using the correction optimized for

the F555W filter. The analysis was performed as above, using the same reference stars. The superposition accuracy to the 1995 reference grid turned out to be accurate within ~ 0.08 pixels per coordinate, (i.e. only slightly less accurate than for the superposition of the F555W data), with no evidence for systematic effects. Also in this case, no significant displacement was measured for the pulsar. Combining F555W and F547M data yields a tighter 3σ proper motion upper limit of 1.2 mas y^{-1}, corresponding to a projected velocity of ~ 290 km s^{-1}. Such a limit, computed using a well-tested, robust algorithm, supersedes the result by Serafimovich et al. (2004), based on a much shorter time baseline.

2.2. Variability of the PWN

The epoch-to-epoch coordinate transformation was then used to rebin and superimpose the images, in order to search for possible variations of the PWN morphology. The resulting images were not corrected for the geometric distortion. However, we note that at the PWN position, imaged at the center of the PC chip, the maximum distorsion correction is ~ 0.05 pixel per coordinate (Anderson & King 2003), i.e. small enough for our goals.

As a first step, we checked consistency of photometry between the observations performed through the same filter at different epochs. To this aim, we compared the count rates from 85 reference stars using simple aperture photometry. The 2005 F555W observations yield systematically lower count rates, with an average 2005–to–1995 ratio of 0.86 (0.07 rms), while the 2005–to–1999 ratio for the F547M observations is 0.90 (0.08 rms). Such values were used to re-normalize the 2005 images.

We started using the 1995 and 2005 F555W images, characterized by a better signal-to-noise. A striking change in the brightest portion of the PWN is immediately apparent when comparing the two images. As noticed by Caraveo et al. (2000) a definite surface brightness maximum is seen in the PWN, South-West to the pulsar optical counterpart. Such a feature, which we will call the "hot spot", is resolved (7.2 pixel FWHM, or 0.081 pc at the LMC distance) and lies $\sim 1\farcs1$ away from the pulsar (0.27 pc) in the 1995 image. Inspection of the 2005 image shows that the hot spot is displaced by $\sim 0\farcs5$ in the SW direction with respect to its location in 1995. This is apparent from Fig. 1, where the two images are compared. Fitting a gaussian function to the hot spot profile, we estimated that the feature moved by $0\farcs46 \pm 0\farcs02$, or 0.11 pc at the LMC distance, corresponding to a velocity of ~ 0.037c assuming simple linear motion.

The apparent displacement of the hot spot corresponds to a very large local variation in the PWN surface brightness. Using a 8×8 pixel aperture ($\sim 0\farcs36 \times 0\farcs36$) centered on the

1995 hot spot position, the count rate is seen to decrease by $25 \pm 2\%$ between 1995 and 2005 (the uncertainty does not account for systematic errors in the image renormalization). We have computed the ratio of the 2005 to the 1995 surface brightness using the same 8×8 pixel aperture, selecting 200 positions to cover the whole PWN (within $\sim 2\farcs5$ from the pulsar). Such an exercise proved that the region of the hot spot is by far the most active part of the PWN. The observed r.m.s. variability on the above 200 PWN regions is $\sim 8\%$, which reduces to $\sim 4\%$ when considering only the brightest 100 regions. Of course, the possible systematics involved in the 2005 to 1995 renormalization do not affect such a conclusion.

The hot spot is clearly seen in the image collected in 2005 with the F547M filter, at a position consistent with the one apparent in the F555W filter. The ratio of the 2005 F547M and F555W images does not show any significant feature at the hot spot position, which suggests the hot spot emission to be dominated by continuum. Indeed, considering a 4 pixel radius aperture centered at the hot spot, we estimated the ratio of the observed background-subtracted count rates to be 0.4 ± 0.1. This is fully consistent with an expected value of 0.45, evaluated with the WFPC2 ETC[3], assuming a power-law spectrum of spectral index $\alpha = 1.6$[4].

Thus, we can use the 1999 F547M image (see Fig.1 of Serafimovich et al. 2004) to constrain the position of the hot spot at a third epoch. Results are shown in Fig. 2. The hot spot peak in 1999 lies $\sim 0\farcs38$ West of its 1995 position, while in 2005 it is seen $\sim 0\farcs33$ South of its 1999 position. The hot spot morphology is also seen to vary, the feature being more extended in 1999. Such results argue against a simple outward motion of the feature and prove a dramatic variability of the PWN in the SW region.

The detection of large time variability in the PWN of PSR B0540-69 makes its similarity with the Crab Nebula even more compelling. Thus, it seems natural to compare in some detail the optical phenomenology of the two systems. The hot spot in the PSR B0540-69 PWN is definitely larger and more distant from the pulsar than the bright, highly variable "wisps" seen in the Crab Nebula (Hester et al. 1995, 2002). It is somewhat reminiscent (as for physical dimensions, distance to the pulsar and temporal behaviour) of a large, roughly arc-shaped structure in the outer Crab nebula, first noticed in the optical by Hester et al. (1995) because of its outstanding variability on a time scale of 6 years (see their Figure 12d). Such a feature is also prominent and highly variable at radio wavelengths (see Fig.2 of Bietenholz et al.

[3]http://www.stsci.edu/hst/wfpc2/software/

[4]Serafimovich et al. (2004) in their spatially-resolved study of the PWN spectrum used a region ("area 2") encompassing the hot spot. Emission from such a region, largely contributed by the hot spot, is consistent with a power law of spectral index 1.6 ± 0.4.

2004). While the nature of such feature is not understood, it is almost certainly related to energy outflows in the counter-jet channel of the Crab PWN (Bietenholz et al. 2004). Complex interactions between the PWN and the surrounding ejecta filaments are also seen in such a region, roughly corresponding to the inner portion of the Norteastern "bay" (Michel et al. 1991; Hester et al. 1995). We retrieved and inspected HST/WFPC2 images of the Crab collected in 1994 and in 2001 through the F547M filter. We found the outer feature to show a variability consistent to the one reported by Hester et al. (1995), corresponding to a local surface brightness variation of order 25%, very similar to the hot spot of PSR B0540-69. We also note that, rescaled at the LMC distance, the variability in the inner nebula (wisps and torus) would be difficult to detect, while the variability of the outer structure would be outstanding.

Coming back to PSR B0540-69, the hot spot lies in the region of the PWN tentatively identified as an equatorial torus by Gotthelf & Wang (2000). The large variability of the feature, coupled to the PWN asymmetry with respect to the pulsar position, as well as the comparison with the case of the Crab, may point to an alternative scenario in which the northeast-southwest axis corresponds to the direction of a pulsar jet/counterjet. This may also be supported by the observation that other PWNe do show (in X-rays) the largest variability along the jet direction, with apparent complex motion of bright blobs, although on shorter time scales (e.g. for PSR B1509-58 and Vela, Delaney et al. 2006; Pavlov et al. 2003) as well as on a smaller physical scale (in Vela, Pavlov et al. 2003). However, no firm conclusions may be drawn based on current data.

3. Conclusions

With the discovery of significant variations in its PWN emission, PSR B0540-69 shares one more characteristic with the Crab pulsar. Moreover, our multi-epoch study of PSR B0540-69 yielded a new assessment of the pulsar proper motion, setting an upper limit of 290 km s^{-1}.

Upcoming WFPC2 observations of PSR B0540-69 will allow us to monitor the PWN morphology, while lowering the measurable velocity to $\sim$ 220 km s^{-1}. The new HST data will be very important to shed light on the geometry and dynamic of the system. High-resolution HST polarimetric mode observations, to be collected in the same program, will offer unvaluable clues in order to understand the overall structure of the PWN and its complex interaction with the cage of filamentary ejecta. PSR B0540-69 will possibly become a unique extra-galactic laboratory to study and understand the variability and evolution of young PWN systems.

This work has been partially supported by the Italian Space Agency (ASI) and INAF through contract ASI/INAF I/023/05/0. ADL acknowledges an ASI fellowship.

REFERENCES

Anderson, J., & King, I.R., 2003, PASP 115, 113

Anderson, J., & King, I.R., 1999, PASP 111, 1095

Bietenholz, M.F., Hester, J.J., Frail, D.A., Bartel, N., 2004, ApJ 615, 794

Caraveo, P.A., De Luca, A., Mignani, R.P., Bignami, G.F., 2001, ApJ 561, 930

Caraveo, P.A., Mignani, R.P., De Luca, A., Wagner, S., Bignami, G.F., 2000, in "A decade of HST science, poster papers", ed. by Livio M., Noll, K. and Stiavelli., M., Baltimore, ND: Space Telescope Science Institute, p.9, astro-ph/0009035

Caraveo, P.A., Mignani, R.P., 1999, A&A 344, 367

Caraveo, P.A., Mignani, R.P., Bignami, G.F., 1998, MmSAI 69, 1061

Caraveo, P.A., Bignami, G.F., Mignani, R., Taff, L.G., 1996, ApJ 461, L91

Caraveo, P.A., Bignami, G.F., Mereghetti, S., Mombelli, M., 1992, ApJ 395, L103

Chanan, G.A., & Helfand, D.J., 1990, ApJ 352, 167

De Luca, A., Mignani, R.P., Caraveo, P.A., 2000, A&A 354, 1011

Delaney, T., Gaensler, B.M., Arons, J., Pivovaroff, M.J., 2006, ApJ 640, 929

Dodson, R., Legge, D., Reynolds, J.E., McCulloch, P.M., 2003, ApJ 596, 1137

Ebeling, H., White, D.A., Rangarajan, F.V.N., 2006, MNRAS 368, 65

Gotthelf, E.V., & Wang, Q.D., 2000, ApJ 532, L117

Hester, J.J., Scowen, P.A., Sankrit, R., et al., 1995, ApJ 448, 240

Hester, J.J., Mori, K., Burrows, D., et al., 2002, ApJ 577, L49

Kaaret, P., Marshall, H.L., Aldcroft, T.L., et al., 2001, ApJ 546, 1159

Manchester, R.N., Mar, D.P., Lyne, A.G., Kaspi, V.M., Johnston, S., 1993, ApJ 403, L29

Michel, F.C., Scowen, P.A., Dufour, R.J., 1991, ApJ 368, 463

Middleditch, J., & Pennypacker, C., 1985, Nature 313, 659

Mignani, R.P., De Luca, A., Caraveo, P.A., 2000, ApJ 543, 318

Morse, J.A., Smith, N., Blair, W.P., et al., 2006, ApJ 644, 188

Ng, C-Y., Romani, R.W., 2006, ApJ 644, 445

Pavlov, G.G., Teter, M.A., Kargaltsev, O., Sanwal, D., 2003, ApJ 591, 1157

Petre, R., Hwang, U., Holt, S.S., Safi-Harb, S., Williams, R.M., 2007, ApJ 662, 988

Serafimovich, N.I., Shibanov, Y.A., Lundqvist, P., Sollerman, J., 2004, A&A 425, 1041

Seward, F.D., Harnden, F.R., Jr, Helfand, D.J., 1984, ApJ 287, L19

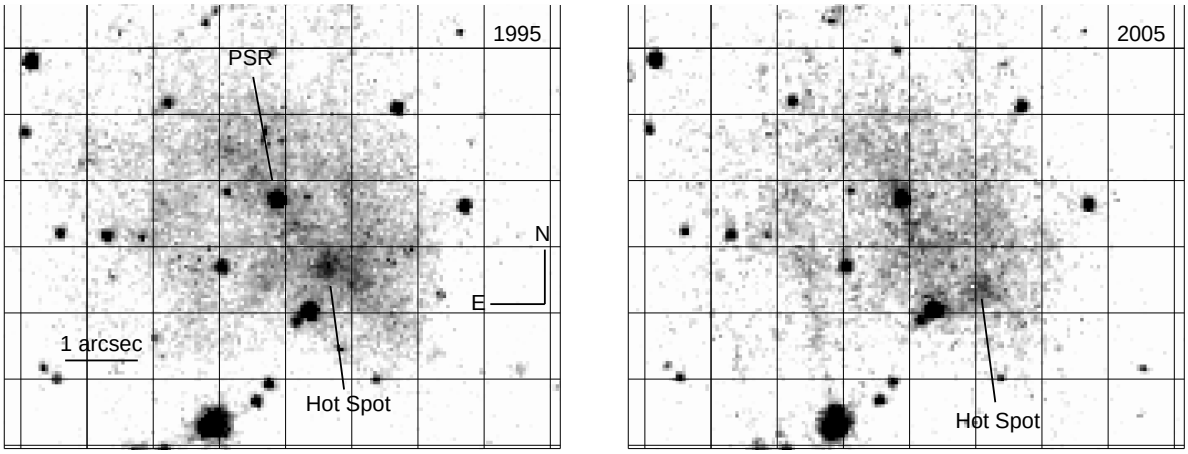

Fig. 1.— The field of PSR B0540-69 as observed with HST/WFPC2 through the F555W filter in 1995 (600 s) and in 2005 (480 s). Pixel size is 0.″0455. The pulsar optical counterpart, as well as the brightest feature of the PWN (the "Hot Spot") are marked. A grid (20 pixel spacing, corresponding to 0.″91) is overplotted to better visualize the apparent displacement of the "Hot Spot".

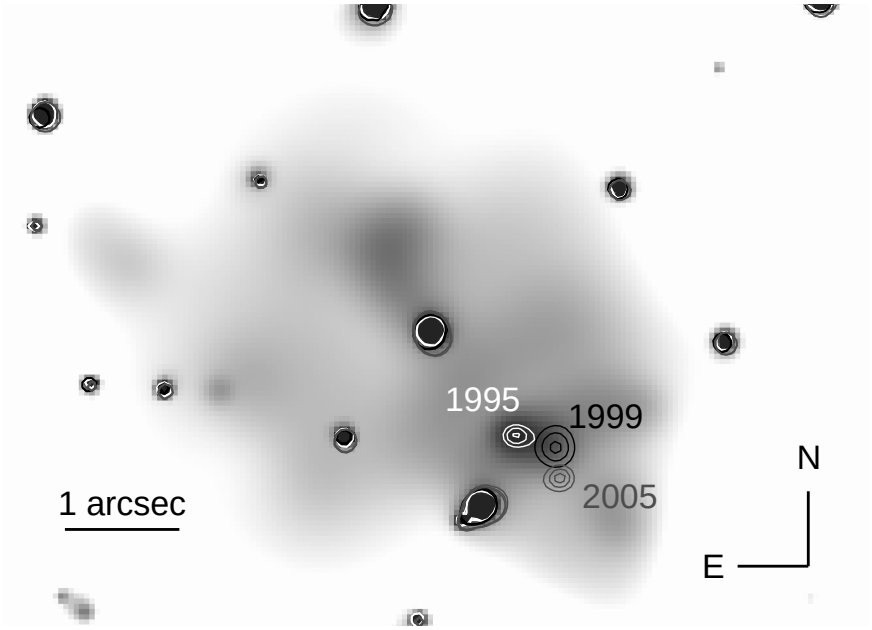

Fig. 2.— The inner field of PSR B0540-69 as observed in 1995 through the F555W filter is shown, after adaptive gaussian smoothing of the HST/WFPC2 image. The *asmooth* algorithm by Ebeling et al. (2006) has been used, setting the minimum S/N threshold to 10 and using a maximum smoothing kernel of 10 pixels. Isophotal contours to mark the hot spot peak (corresponding to 99%, 95% and 99% of the maximum of the PWN surface brightness) are plotted in white. Contours generated using the same criteria for the 1999 and 2005 images are overplotted. The displacement of the hot spot is apparent.